

^{59}Co NMR experiment as a probe of electron doping in $\text{Co}_2\text{FeAl}_{1-x}\text{Si}_x$ Heusler alloysM. Wójcik,¹ E. Jedryka,¹ H. Sukegawa,² T. Nakatani,² and K. Inomata²¹*Institute of Physics, Polish Academy of Sciences, 02-668 Warsaw, Poland*²*National Institute for Materials Science, 1-2-1 Sengen, Tsukuba 305-0047, Japan*

(Received 7 November 2011; published 1 March 2012)

A systematic ^{59}Co NMR study has been carried out at 4.2 K in a series of quaternary $\text{Co}_2\text{FeAl}_{1-x}\text{Si}_x$ polycrystalline bulk Heusler alloys ($x = 0, 0.3, 0.5, 0.7, 1$). It was shown that the effect of Si substitution consists in a significant modification of ^{59}Co hyperfine field and that this modification is mainly due to the contribution from s valence electron polarization, suggesting a shift of the Fermi energy level inside the half-metallic gap. This observation supports the theoretical predictions that the Fermi-level position in Co_2FeZ Heusler alloys can be effectively tuned by varying the composition of the Z sublattice.

DOI: [10.1103/PhysRevB.85.100401](https://doi.org/10.1103/PhysRevB.85.100401)

PACS number(s): 71.20.Lp, 76.60.Jx, 76.60.Lz, 72.25.Ba

Co-based Heusler compounds^{1–4} denoted by the general formula Co_2YZ (where Y is a transition metal, e.g., Fe, Mn, whereas Z is a main group element, e.g., Si, Al, Ge), have attracted scientific and technological interest due to their potential applications as materials for magnetoelectronic devices. This interest is driven by the exceptional electronic structure found in these compounds. Several of them exhibit a complete spin polarization at the Fermi energy (ε_F), meaning that they behave as a metal for electrons of one spin direction and as an insulator for the other.⁵ For practical applications the most interesting compositions are Co_2FeSi (CFS), which has the highest magnetic moment per formula unit ($6\mu_B$) (Ref. 6) among Heusler alloys and Co_2FeAl (CFA) with a magnetic moment of $5\mu_B$.⁷ Their Curie temperature is very high ($T_C = 1100$ K for CFS and 980 K for CFA, respectively), making them the materials of choice for room-temperature (RT) applications. Spin polarization at low temperatures has been theoretically predicted to be close to 100% for these two compounds^{8,9} (see Fig. 1). Unfortunately, their complex crystal structure consisting of four interpenetrating fcc sublattices ($L2_1$ structure—see Fig. 2) makes them prone to chemical disorder, which is a potential source for the loss of half metallicity.^{10–12} However, even in the case of perfect structural ordering, the specific features of the band structure can also lead to a reduced polarization at finite temperatures. Depending on the Fermi-level (ε_F) position inside the gap, two scenarios are possible, as illustrated in Fig. 1. In the case of CFA, where the ε_F is located near the top of the conduction band, occupation of the minority states due to the Fermi-Dirac distribution may reduce spin polarization. On the other hand, in CFS, where the Fermi level is close to the bottom of the conduction band, the energy gap may get closed by thermal excitations (magnons). A desired solution to this problem would consist in stabilizing the half-metallic properties by fixing the Fermi energy well within the half-metallic band gap. Calculations of the electronic structure in $\text{Co}_2\text{FeAl}_{1-x}\text{Si}_x$ (CFSA) Heusler alloys show that these compounds obey the Slater-Pauling rule^{13,14} and the magnetic moment per formula unit (M_t) varies linearly with the number of valence electrons (Z_{val}) of the system, and thus $M_t = Z_{\text{val}} - 24$. Consequently, the addition of an extra valence electron by substituting $\text{Al}([\text{Ne}]3s^23p^1)$ with $\text{Si}([\text{Ne}]3s^23p^2)$ can be regarded as electron doping of the majority-spin band leading to a virtual shift

of the Fermi level inside the gap of the minority-spin band.^{12,15} And indeed, by replacing 50% of Si for Al, a unique Heusler alloy with a composition $\text{Co}_2\text{FeAl}_{0.5}\text{Si}_{0.5}$ has been developed, making it possible to fabricate a tunnel magnetoresistance (TMR) junction with a good temperature stability—the TMR value varied only from 390% at 5 K to 220% at RT.^{16,17} Recently it has been shown that CFSA thin films reveal a high spin polarization at room temperature (polarization of 0.91) and show very weak temperature dependence of conduction electron spin polarization.¹⁸

In order to get an experimental insight into the state of polarization of the conduction electrons in the mixed CFSA system, we have carried out a systematic ^{59}Co NMR study in a series of quaternary $\text{Co}_2\text{FeAl}_{1-x}\text{Si}_x$ compounds ($x = 0, 0.3, 0.5, 0.7, 1$). We make use of the well-known fact that in ferromagnetic materials the NMR frequency probes directly the value of the hyperfine field (HF), which reflects the spatial distribution of electron spins around the nucleus. In particular, the hyperfine field is extremely sensitive to a small spin polarization of the $4s$ valence electrons and therefore it should make it possible to detect the changes of their contribution to the magnetic moment induced in CFSA. In this way one should be able to verify whether indeed a substitution of Si for Al leads to the change of electron count in the majority-spin band of the Co_2FeZ structure.

Experimental details. A series of $\text{Co}_2\text{FeAl}_{1-x}\text{Si}_x$ polycrystalline bulk samples ($x = 0, 0.3, 0.5, 0.7, 1$) have been prepared by arc-melting under Ar atmosphere, followed by an appropriate annealing procedure. The samples were thoroughly characterized for their structural and magnetic properties—the details of sample preparation and characterization are given elsewhere.¹⁹

^{59}Co NMR spin-echo signals were recorded every 0.5 MHz using an automated, phase sensitive spectrometer.²⁰ The experiments have been carried out at 4.2 K in the absence of an external magnetic field, at several values of rf excitation field. All the NMR spectra have been corrected for the intrinsic NMR enhancement factor following the Panissod protocol^{21,22}—this procedure corrects for the inhomogeneities of the NMR enhancement factor within the studied sample and ensures that the relative intensities in the corrected NMR spectrum are proportional only to the number of nuclei resonating at a given NMR frequency.

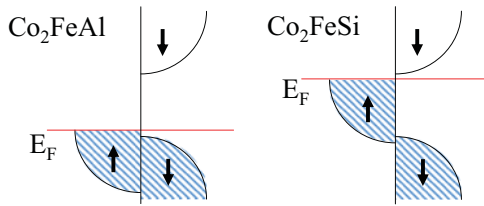


FIG. 1. (Color online) Schematic illustration of the electronic structure around the Fermi energy for Co_2FeAl and Co_2FeSi emphasizing the difference in their respective Fermi-level position inside the gap for the minority-spin states.

Results and discussion. Heusler alloys denoted by a general formula X_2YZ crystallize in a cubic $L2_1$ structure with the corresponding $Fm\bar{3}m$ space group. The $L2_1$ structure consists of four fcc interpenetrating sublattices that are offset along the $[111]$ direction with the following site occupancy: $X(0,0,0)$, $Y(\frac{1}{4},\frac{1}{4},\frac{1}{4})$, $X(\frac{1}{2},\frac{1}{2},\frac{1}{2})$, and $Z(\frac{3}{4},\frac{3}{4},\frac{3}{4})$ (Fig. 2). In the case of $\text{Co}_2\text{FeSi(Al)}$ compounds, Co atoms occupy two sublattices denoted as X , whereas Fe and Si(Al) atoms occupy sublattices Y and Z , respectively. The highly ordered $L2_1$ structure for Co_2FeZ may transform to $B2$ or further to an $A2$ structure depending on a degree of atomic site disorder. The symmetry lowers to $B2$ if Fe and Z atoms are evenly distributed over Y and Z sublattices. In the case of a random atomic mixing between X and Y or X and Z sublattices, respectively, the symmetry lowers to DO_3 . Finally, the $A2$ symmetry implies that all sublattices become equally populated by all kinds of atoms.

Figure 3 presents the ^{59}Co NMR spectra recorded at 4.2 K from the entire series of studied samples. One can readily notice a striking difference between the spectral shapes in the two extreme compositions. While the undoped CFS displays a single NMR line, in the case of the spectrum from the undoped CFA a well-resolved structure of equally spaced ($\Delta f \cong 32$ MHz) satellite lines is observed on both sides of the main ($L2_1$) NMR line. Obviously, in the case of the perfect $L2_1$ structure all Co atoms have identical nearest-neighbor (nn) environment (Fig. 2), and this should give rise to a single NMR line, just as it is observed in CFS. The presence of a satellite structure in CFA indicates a certain distribution

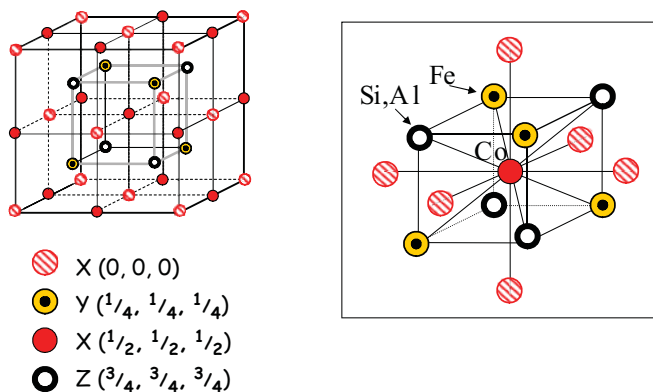


FIG. 2. (Color online) Left: Atomic arrangement of the four sublattices ($X = \text{Co}$, $Y = \text{Fe}$, $X = \text{Co}$, $Z = \text{Al}$, Si) in the perfect $L2_1$ structure. Right: Nearest-neighbor environment of Co atoms in this structure.

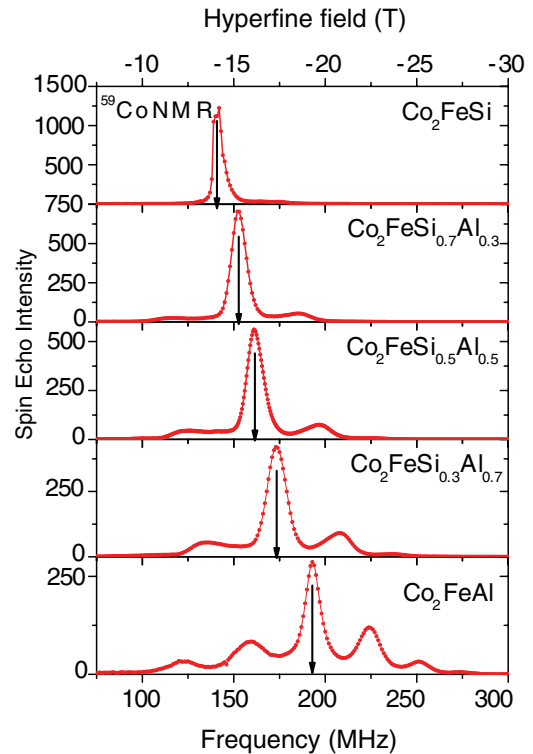


FIG. 3. (Color online) ^{59}Co NMR spectra recorded for $\text{Co}_2\text{FeAl}_{1-x}\text{Si}_x$ polycrystalline bulk Heusler alloys at 4.2 K. The arrows indicate the NMR line corresponding to Co atoms in the perfect $L2_1$ environment [tetrahedrally arranged 4Fe and 4Al(Si) nearest neighbors].

of local environments, which modify the hyperfine field on the studied Co nucleus via the transferred hyperfine field component, as demonstrated in the phenomenological model of hyperfine fields in metallic alloys.²³

In view of the absence of Si admixture in Co_2FeAl composition, this satellite structure is readily attributed to the random intermixing of Fe and Al ions over their respective sublattices, creating a number of Fe_{Al} and Al_{Fe} antisites. A detailed analysis of this structural disorder observed in CFA has been presented in Ref. 24. Interestingly, the present results, obtained in a series of intermediate CFSAs compositions, show no influence of the different nn environments (naturally created upon replacement of some Al ions by Si) on the shape of NMR spectrum—no additional satellites appear. To the contrary, the intensity of the satellite lines visibly decreases, suggesting that Si stabilizes the desired $L2_1$ structure, which supports the theoretical predictions that the $3(s,p)$ orbitals of Si make a stronger hybrid bond with the $3d$ transition-metal orbitals in the CFS structure.¹⁵ The amount of Fe-Al antisites, computed in frames of the model described in Ref. 24, gradually decreases with increasing content of Si, as shown in Fig. 4. The main effect of silicon substitution consists in a systematic shift of the entire ^{59}Co NMR spectrum toward lower frequencies, pointing out that (Al-Si) replacement has a global (rather than local) effect on the electronic structure and thus on the value of the ^{59}Co hyperfine field. The frequency position of the main ($L2_1$) line for the entire range of compositions decreases in a quasilinear way from 193 MHz in CFA to

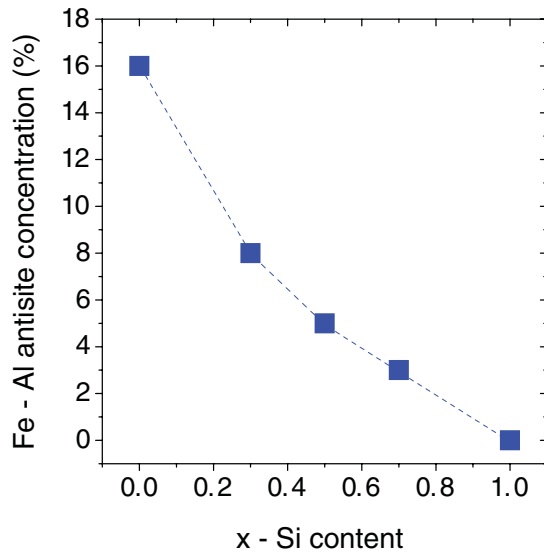


FIG. 4. (Color online) Fe-Al antisite concentration as a function of Si content in $\text{Co}_2\text{FeAl}_{1-x}\text{Si}_x$.

139 MHz in CFS. The corresponding ^{59}Co hyperfine field varies thus between -19.1 and -13.76 T, as presented in Fig. 5. To understand this, one has to consider the origin of different contributions to the hyperfine field, which in the case of ferromagnetic $3d$ metals consists mainly of the Fermi contact term²⁵ $H_{\text{hf}} = \frac{8\pi}{3} \mu_B^2 m(0)$, where $m(0)$ denotes the spin density of s electrons at the nucleus. Two main mechanisms, originating respectively from the core and from the valence electrons, contribute to the contact Fermi term. The first is known as *exchange polarization* $m(0) \propto (|\psi_{ns\uparrow}(0)|^2 - |\psi_{ns\downarrow}(0)|^2)$ and relates $m(0)$ to the difference of spin-up and spin-down s electron densities at the nucleus due to the s - d exchange and phenomenologically can be regarded as proportional to the on-site magnetic moment. The second mechanism, known as *population polarization* $m(0) \propto (n_{4s\uparrow} - n_{4s\downarrow})$ relates $m(0)$ to the difference in population of $4s$ electrons with spin up and spin down near the ε_F and, consequently, to the magnetic moment of $4s$ electrons. These two distinct mechanisms give rise to the hyperfine field originating from the core electrons (H_{core}) and to the valence electrons (H_{valence}), respectively. The former can be computed assuming that the observed increase of the total magnetic moment per formula unit (from $5\mu_B$ in CFA to $6\mu_B$ in CFS) can be attributed mainly to the variation of Co moment. This assumption is supported by the electronic structure calculations, which give the values of Co magnetic moments $\sim 1.1\mu_B$ in CFA and $\sim 1.5\mu_B$ in CFS and the corresponding values of Fe magnetic moments $\sim 2.8\mu_B$ and $\sim 3.0\mu_B$, respectively.² This insignificant variation of Fe magnetic moment is consistent with the observed constant spacing of the satellite lines due to the Fe-Al antisites, as described above. In the analysis of the experimental data the values of H_{core} in particular samples have been computed assuming a linear variation of Co magnetic moment with the Si content and by using the expression $H_{\text{core}} = A\mu(\text{Co})$, where the interaction constant was approximated as $A = -10 \text{ T}/\mu_B$.²⁵ Thus computed values of H_{core} have been used to estimate the H_{valence} contribution as the difference between the H_{exp} and H_{core} . The results are plotted in Fig. 5, where the H_{core}

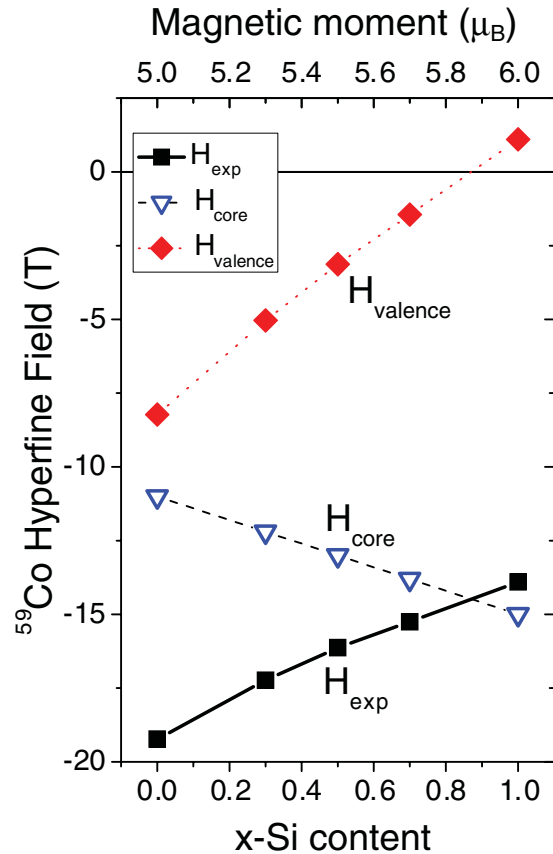


FIG. 5. (Color online) Experimental ^{59}Co hyperfine fields (H_{exp}) in $\text{Co}_2\text{FeAl}_{1-x}\text{Si}_x$ corresponding to Co atoms located in a perfect $L2_1$ environment as well as the respective contributions from the core s shell ($1s, 2s, 3s$) electrons (H_{core}) and the $4s$ valence electrons (H_{valence}).

decreases from -11 T for CFA to -15 T for CFS—the slope of this variation is thus opposite to the experimentally observed increase of the total hyperfine field. On the other hand, the resulting almost linear change of H_{valence} has a positive slope, entailing the change of sign of this term: It varies from -8.1 T in CSA to 0 for x around 0.8–0.9 and becomes positive and equal to $+1.2$ T for CFS. This rough analysis clearly points out that the experimentally observed variation of ^{59}Co H_{hf} upon alloying mainly reflects the variation of the valence electron contribution. The previously evoked hyperfine field mechanism predicts that H_{valence} is proportional to the magnetic moment of $4s$ electrons of Co and this allows one to relate it to the spin-polarized density of states. This relation has been independently confirmed by Deb *et al.* in hyperfine field calculations for the series of Cu_2MnAl , Ni_2MnSn , and Co_2FeGa Heusler alloys.²⁶ The positive slope of valence electron contribution to the hyperfine field means that the population of $4s$ electrons with “spin up” increases faster than the population with “spin down” and above $x \cong 0.9$ the total $4s$ spin polarization becomes positive. Assuming the rigid band model (suggested by the results of the electronic structure calculations), this means that the additional electron introduced by substituting $\text{Al}([\text{Ne}]3s^23p^1)$ with $\text{Si}([\text{Ne}]3s^23p^2)$ enters preferentially the majority “spin-up” valence band, which is consistent with the theoretical scenario predicting that the

electron dopes the majority-spin band, leading to a virtual shift of the Fermi level inside the gap of the minority-spin band.

Conclusions. In conclusion, we have shown that the effect of Si substitution in $\text{Co}_2\text{FeAl}_{1-x}\text{Si}_x$ Heusler alloys consists in a significant modification of the ^{59}Co hyperfine field and that this modification is mainly due to the contribution from valence electron polarization, suggesting a shift of the Fermi energy inside the half-metallic gap. This observation supports the theoretical predictions that the Fermi-level position in Co_2FeZ Heusler alloys can be effectively tuned by varying

the composition of the Z sublattice and is experimental confirmation of these calculations. More generally, these materials are particularly interesting as a working example of the applicability of computational physics to effectively design new spintronic materials by manipulating the position of the Fermi level.

Acknowledgment. This work has been supported in part by a grant from by the Ministry of Sciences and Higher Education of Poland under the Research Project No. 4531/B/T02/2010/38 for the years 2010–2013.

-
- ¹C. Felser, G. H. Fecher, and B. Balke, *Angew. Chem., Int. Ed.* **46**, 668 (2007).
- ²B. Balke, S. Wurmehl, G. H. Fecher, C. Felser, and J. Kübler, *Sci. Technol. Adv. Mater.* **9**, 014102 (2008).
- ³K. Inomata, S. Okamura, A. Miyazaki, M. Kikuchi, N. Tezuka, M. Wojcik, and E. Jedryka, *J. Phys. D: Appl. Phys.* **39**, 816 (2006).
- ⁴K. Inomata, N. Ikeda, N. Tezuka, R. Goto, S. Sugimoto, M. Wojcik, and E. Jedryka, *Sci. Technol. Adv. Mater.* **9**, 014101 (2008).
- ⁵J. Kübler, A. R. Williams, and C. B. Sommers, *Phys. Rev. B* **28**, 1745 (1983).
- ⁶S. Wurmehl, G. H. Fecher, H. C. Kandpal, V. Ksenofontov, C. Felser, H. J. Lin, and J. Morais, *Phys. Rev. B* **72**, 184434 (2005).
- ⁷J. M. De Teresa, D. Serrate, R. Cordoba, and S. M. Yusuf, *J. Alloys Compd.* **450**, 31 (2008).
- ⁸H. C. Kandpal, G. H. Fecher, C. Felser, and G. Schonhense, *Phys. Rev. B* **73**, 094422 (2006).
- ⁹Y. Miura, K. Nagao, and M. Shirai, *Phys. Rev. B* **69**, 144413 (2004).
- ¹⁰I. Galanakis, K. Özdoğan, B. Aktas, and E. Şaşıoğlu, *Appl. Phys. Lett.* **89**, 042502 (2006).
- ¹¹K. Özdoğan, B. Aktas, I. Galanakis, and E. Şaşıoğlu, *J. Appl. Phys.* **101**, 073910 (2007).
- ¹²Z. Gersi and K. Hono, *J. Phys. Condens. Matter* **19**, 326216 (2007).
- ¹³I. Galanakis, P. H. Dederichs, and N. Papanikolaou, *Phys. Rev. B* **66**, 174429 (2002).
- ¹⁴G. H. Fecher, H. C. Kandpal, S. Wurmehl, C. Felser, and G. Schonhense, *J. Appl. Phys.* **99**, 08J106 (2006).
- ¹⁵G. H. Fecher and C. Felser, *J. Phys. D: Appl. Phys.* **40**, 1582 (2007).
- ¹⁶N. Tezuka, N. Ikeda, S. Sugimoto, and K. Inomata, *Appl. Phys. Lett.* **89**, 252508 (2006).
- ¹⁷N. Tezuka, N. Kieda, S. Sugimoto, and K. Inomata, *Jpn. J. Appl. Phys., Part 2* **46**, L454 (2007).
- ¹⁸R. Shan, H. Sukegawa, W. H. Wang, M. Kodzuka, T. Furubayashi, T. Ohkubo, S. Mitani, K. Inomata, and K. Hono, *Phys. Rev. Lett.* **102**, 246601 (2009).
- ¹⁹T. M. Nakatani, A. Rajanikanth, Z. Gersi, Y. K. Takahashi, K. Inomata, and K. Hono, *J. Appl. Phys.* **102**, 033916 (2007).
- ²⁰S. Nadolski, M. Wojcik, E. Jedryka, and K. Nesteruk, *J. Magn. Magn. Mater.* **140-144**, 2187 (1995).
- ²¹P. Panissod, NATO ASI Ser., Ser. 3 **48**, 225 (1997).
- ²²M. Malinowska, M. Wojcik, S. Nadolski, E. Jedryka, C. Mény, P. Panissod, M. Knobel, A. D. C. Viegas, and J. E. Schmidt, *J. Magn. Magn. Mater.* **198-199**, 599 (1999).
- ²³C. Mény, E. Jedryka, and P. Panissod, *J. Phys.: Condens. Matter* **5**, 1547 (1993).
- ²⁴K. Inomata, M. Wojcik, E. Jedryka, N. Ikeda, and N. Tezuka, *Phys. Rev. B* **77**, 214425 (2008).
- ²⁵Hisazumi Akai, Masako Akai, S. Blugel, B. Drittler, H. Ebert, Kiyoyuki Terakura, R. Zeller, and P. H. Dederichs, *Prog. Theor. Phys. Suppl.* **101**, 11 (1990).
- ²⁶A. Deb, M. Itou, Y. Sakurai, N. Hiraoka, and N. Sakai, *Phys. Rev. B* **63**, 064409 (2001).